THE
PHYSICAL REVIEW

A journal of experimental and theoretical physics established by E. L. Nichols in 1893

SECOND SERIES, VOL. 180, NO. 3 15 APRIL 1969

The Tight-Binding and the Nearly-Free-Electron Approach to Lattice Electrons in External Magnetic Fields

DIETER LANGBEIN
James Franck Institute, University of Chicago, Chicago, Illinois
and
Battelle Institute, Frankfurt/Main, Germany
(Received 19 June 1968)

The energy structure for lattice electrons in an external magnetic field is treated by extension of either the tight-binding or the nearly-free-electron method. The secular problems resulting from both methods are identical, if the coupling integrals and the real lattice characterizing the tight-binding method are interchanged with the Fourier integrals and the orbit lattice characterizing the nearly-free-electron method. A Bloch-type transformation reducing these essentially two-dimensional secular problems to one dimension is performed, following the procedure introduced in a preceding paper. For rational fluxes $2\pi N/M$ per lattice cell, an even finite secular determinant is left, yielding a splitting of each zero-field band into M subbands. Total agreement between the level structures resulting from the two approaches is found. The relation of these structures to the de Haas–van Alphen periods in the case of magnetic breakdown is discussed.

I. INTRODUCTION

THE tight-binding and the nearly-free-electron methods are known to represent opposite approaches to the electronic-band structure in crystals. On the other hand, they too have much in common. The tight-binding method starts from electron states localized in real space at different lattice sites. The splitting of the atomic levels into bands results from the migration of electrons between neighboring atoms, that is, from coupling integrals between the lattice potential and electron orbits at different lattice sites. The nearly-free-electron method, on the other hand, starts from plane waves, that is, from electron states localized in reciprocal space. The formation of gaps in the corresponding continuous energy spectrum results from Bragg reflections of the electrons into neighboring sites of the reciprocal lattice, that is, from Fourier components of the lattice potential corresponding to reciprocal lattice sites.

It is the objective of this paper to show that this analogy can be extended successfully to include problems which also involve an external magnetic field. The methods used so far in the nearly-free-electron method may indeed be understood as tight-binding methods in reciprocal space. An extension of both approaches easily provides full information on the energy-band structure for arbitrary lattice potentials and fields. Explicit calculations are performed for magnetic fields parallel to a tetragonal or hexagonal axis of the lattice.

The first application of the tight-binding method to lattice electrons in magnetic fields goes back to Peierls.[1] He has proved that the Hamiltonian can be replaced by the operator $E(\hat{k})$, where $E(\mathbf{k})$ is the electron energy for vanishing field and $\hat{k}$ obeys the commutation relation $[\hat{k},\hat{k}]=i\mathbf{B}$. Successful tight-binding calculations of the magnetic-band structure were performed by Harper[2] and by Brailsford.[3] Using the Peierls $E(\hat{k})$ operator, these authors approximate the eigenfunctions by the WKB method. The continuous zero-field energy bands are found to split up into broadened Landau levels, the broadening decreasing exponentially at the band edges. A direct tight-binding solution of the Hamiltonian for finite orthorhombic crystals was given by Gerlach and Langbein,[4] in order to show explicitly the gradual formation of Landau levels with increasing crystal thickness. The secular determinant for the limit of infinite crystals can be reduced to a finite determinant of order M, whenever the magnetic flux ϕ per unit cell divided by 2π takes a rational value N/M. The eigenvalues then form M subbands, whose width increases towards the center of the level system.

[1] R. Peierls, Z. Physik **80**, 763 (1933).
[2] P. G. Harper, Proc. Phys. Soc. (London) **A68**, 874 (1955).
[3] A. D. Brailsford, Proc. Phys. Soc. (London) **A70**, 275 (1957).
[4] E. Gerlach and D. Langbein, Phys. Rev. **145**, 449 (1966).

While experimentally available magnetic fields change the localized tight-binding orbitals only slightly, they mean a strong perturbation to the free-electron orbitals used in the nearly-free-electron method. Instead of plane waves and a continuous energy spectrum, one now has localized Landau states and discrete, equidistant energies. Calculations of the energy spectrum in lattices starting from Landau states seemed to have little interest, until Cohen and Falicov[5] pointed out that an occasional remaining of the electrons in these orbits instead of following the zero-field energy contours can produce new quantized orbits responsible for some high-frequency de Haas–van Alphen oscillations in magnesium. Since with increasing localization in real space the electrons become more smeared out in k space, they will more likely tunnel through the small regions of higher energy caused by the Bragg reflections. The low-field approach to this breakdown phenomenon was given by Blount.[6] A rather general method has been introduced by Pippard.[7,8] He assumes the electrons to be most of the time closely confined to well-defined paths in real space, but allows switching from one path to another when the conditions for a Bragg reflection are satisfied. The centers of all orbits thus connected are found to form a lattice similar to the real lattice, but $2\pi/\phi$ times as big. It is generally referred to as orbit lattice. Pippard has applied this model to calculate the broadening of Landau levels for fluxes per unit cell equal to $2\pi/M$, M integer, so that all centers of the orbit lattice are identically situated on the real lattice. Since the switching probability between equivalent paths is treated as an adjustable parameter, his results can be applied to weak as well as to strong lattice potentials. An extension to rational fluxes $\phi/2\pi=N/M$ was given by Chambers,[9] using a one-dimensional model Hamiltonian introduced by Zak.[10] The bands found by Pippard split up in this case into N subbands.

Turning back to the ideas of the tight-binding method we find that Pippard's model can be interpreted as a one-band tight-binding method in reciprocal space. The orbits discussed are tightly bound to a doubly infinite set of fixed paths in k space; the transitions between them are caused by Bragg reflections, that is, by the Fourier components of the lattice potential. Except for the freely adjustable switching parameter no further systematic changes of the orbits are considered.

In Secs. II and III we set up the basic equations for a multiband tight-binding and nearly-free-electron approach in magnetic fields, respectively. In Sec. IV we calculate in second-order perturbation theory the broadening of Landau levels due to a one-dimensional periodic potential normal to the magnetic field. Application of the resulting electron orbitals to two-dimensional potentials normal to the field (Sec. V) yields a secular determinant which has exactly the same form as that obtained in the tight-binding method. The Fourier components of the lattice potential replace the coupling integrals, and the orbit lattice replaces the real lattice. Each Landau level corresponds to one band. In Sec. VI we reduce this two-dimensional secular problem to a one-dimensional one, by means of the Bloch-type transformation introduced in Ref. 4. The general features of the resulting energy scheme are discussed by performing a graphic perturbation treatment. Assuming rational fluxes $\phi/2\pi=N/M$ per unit cell of the real lattice in Sec. VII, we are left with a finite secular determinant of order M (tight-binding method) or N (nearly-free-electron method). Explicit level schemes are calculated for field directions with tetragonal or hexagonal symmetry and in a nearest orbit approximation. The original tight-binding bands (or Landau levels) split up into M (or N) subbands, arranged in groups of N (or M). They are spaced equidistantly for fluxes $\phi/2\pi$ close to an integer and energies close to a zero-field band edge. The electrons primarily move on orbits surrounding integer fluxes, thus causing discrete levels, and secondly follow the energy contours in k space, thus not fully realizing their zero-field mobility: The over-all bandwidth is narrowed. In Sec. VIII we occupy ourselves with the resulting broadening and structure of the Landau levels. One-dimensional potentials cause merely a broadening, while two-dimensional potentials cause a broadening and a splitting. The period of the broadening depends on the area of overlap between adjacent orbits, and the period of the splitting depends on the area of the unit cell. Both the broadening and the splitting entail matching de Haas–van Alphen frequencies (Sec. IX).

II. BASIC TIGHT-BINDING EQUATIONS

Throughout this paper we will use atomic units, $\hbar=e=m=1$. The magnetic field $\mathbf{B}$ we define relative to the velocity of light c such that the cyclotron frequency simply equals B. In the tight-binding method we use for the magnetic vector potential $\mathbf{A}(\mathbf{r})$ the symmetric gauge

$$\mathbf{A}(\mathbf{r})=\tfrac{1}{2}(\mathbf{B}\times\mathbf{r}). \tag{1}$$

The Schrödinger equation for an electron in a periodic lattice potential $V(\mathbf{r})$ and a homogeneous magnetic field $\mathbf{B}$ then takes the form

$$(H-E)\psi=\{\tfrac{1}{2}[-i\nabla-\tfrac{1}{2}(\mathbf{B}\times\mathbf{r})]^2+V(\mathbf{r})-E\}\psi=0. \tag{2}$$

Denoting an arbitrary set of basis vectors for the real lattice by $\mathbf{a}_i$, we define the reciprocal basis vectors $\mathbf{b}_j$ by

$$\mathbf{a}_i\cdot\mathbf{b}_j=2\pi\delta_{ij}\quad(i,j=1,2,3) \tag{3}$$

and choose the magnetic field $\mathbf{B}$ to be parallel to $\mathbf{a}_3$. This

[5] M. H. Cohen and L. M. Falicov, Phys. Rev. Letters **7**, 231 (1961).
[6] E. I. Blount, Phys. Rev. **126**, 1636 (1962).
[7] A. B. Pippard, Proc. Roy. Soc. (London) **A270**, 1 (1962).
[8] A. B. Pippard, Phil. Trans. Roy. Soc. London **A256**, 317 (1964).
[9] W. G. Chambers, Phys. Rev. **140**, A135 (1965).
[10] J. Zak, Phys. Rev. **136**, A1647 (1964).

restricts $\mathbf{B}$ only slightly, as long as we do not consider $\mathbf{a}_i$ to form a highly symmetric basis. It enables us to separate the Hamiltonian (2) with respect to $\mathbf{a}_3$ by means of the Bloch theorem and to handle (2) throughout the major part of this paper as a two-dimensional differential equation.

For the set of atomic functions or, better, Wannier functions, required for the tight-binding approach we use the notation $\{|\mathbf{a}n\rangle\}$, where $\mathbf{a}$ is an arbitrary lattice vector, $\mathbf{a}=\sum_i \mu_i\mathbf{a}_i$, and n is the band index. We assume them to be equally gauged, by multiplying the zero-field functions by the phase factors $e^{-i\mathbf{r}\cdot\mathbf{A}(\mathbf{a})}$.

Let us, for simplicity, first consider the two-dimensional case, that is, a two-dimensional lattice potential $V(\mathbf{r})$ which varies only in directions normal to the field, and with no variation of $V(\mathbf{r})$ parallel to $\mathbf{B}$. Reserving the notation $\mathbf{a}$ for three-dimensional lattice vectors, we denote two-dimensional lattice vectors normal to $\mathbf{B}$ generally by $\boldsymbol{\alpha}$, with

$$\boldsymbol{\alpha}=\mu_1\mathbf{a}_1+\mu_2\mathbf{a}_2, \quad \mathbf{a}=\boldsymbol{\alpha}+\mu_3\mathbf{a}_3, \tag{4}$$

so that the set of orbitals necessary for the two-dimensional case is $\{|\boldsymbol{\alpha}n\rangle\}$.

In order to solve the Schrödinger equation (2) by the variational principle, we have to calculate the matrix elements of $H-E$ with respect to $|\boldsymbol{\alpha}n\rangle$ and to equate the resulting secular determinant to zero. If we assume the overlap integrals to vanish and use the general gauging relation

$$\langle\mathbf{a}'n'|H-E|\mathbf{a}n\rangle=\langle(\mathbf{a}'-\mathbf{a})n'|H-E|\mathbf{0}n\rangle \times\exp[\tfrac{1}{2}i\mathbf{B}(\mathbf{a}\times\mathbf{a}')], \tag{5}$$

we obtain

$$\langle\boldsymbol{\alpha}'n'|H-E|\boldsymbol{\alpha}n\rangle=(H_n-E)\delta_{n'n}\delta_{\alpha'\alpha}+U_{n'n}(\boldsymbol{\alpha}'-\boldsymbol{\alpha}) \times\exp[\tfrac{1}{2}i\mathbf{B}(\boldsymbol{\alpha}\times\boldsymbol{\alpha}')], \tag{6}$$

where H_n is the expectation value for the KE,

$$H_n=\langle\mathbf{0}n|\tfrac{1}{2}(-i\nabla-\mathbf{A}(\mathbf{r}))^2|\mathbf{0}n\rangle, \tag{7}$$

and $U_{n'n}(\boldsymbol{\alpha})$ is the coupling integral defined by

$$U_{n'n}(\boldsymbol{\alpha})=\langle\boldsymbol{\alpha}n'|V(\mathbf{r})|\mathbf{0}n\rangle. \tag{8}$$

Equation (6) gives the general secular problem for the two-dimensional tight-binding case. The exponential $\exp[\frac{1}{2}i\mathbf{B}(\boldsymbol{\alpha}\times\boldsymbol{\alpha}')]$ shows the most important effect of the magnetic field on a transition of an electron from $|\boldsymbol{\alpha}n\rangle$ to $|\boldsymbol{\alpha}'n'\rangle$ to be a phase shift, which equals half the magnetic flux through the parallelogram spanned by $\boldsymbol{\alpha}$ and $\boldsymbol{\alpha}'$.

Turning to the three-dimensional Hamiltonian (2), we use the same procedure as before, but replace the two-dimensional orbital set $\{|\boldsymbol{\alpha}n\rangle\}$ by Bloch sums $\{|\boldsymbol{\alpha}\theta_3n\rangle\}$ over the three-dimensional orbital set $\{|\mathbf{a}n\rangle\}$. We put

$$|\boldsymbol{\alpha}\theta_3n\rangle=\sum_{\mu_3} e^{-i\mu_3\theta_3}|\mathbf{a}n\rangle, \tag{9}$$

where θ_3 is the wave number for the $\mathbf{a}_3$ direction, or, more exactly, the projection of the wave number in the $\mathbf{b}_3$ direction on $\mathbf{a}_3$. Then, applying (5) once more, we obtain for the matrix elements of $H-E$ with respect to $|\boldsymbol{\alpha}\theta_3n\rangle$

$$\langle\boldsymbol{\alpha}'\theta_3'n'|H-E|\boldsymbol{\alpha}\theta_3n\rangle=\delta(\theta_3'-\theta_3)\{[H_n(\theta_3)-E]\delta_{n'n}\delta_{\alpha'\alpha} +U_{n'n}(\boldsymbol{\alpha}'-\boldsymbol{\alpha},\theta_3)\exp[\tfrac{1}{2}i\mathbf{B}(\boldsymbol{\alpha}\times\boldsymbol{\alpha}')]\}, \tag{10}$$

where $U_{n'n}(\boldsymbol{\alpha},\theta_3)$ is a Bloch sum over coupling integrals for varying μ_3 and fixed $\boldsymbol{\alpha}$,

$$U_{n'n}(\boldsymbol{\alpha},\theta_3)=\sum_{\mu_3} e^{i\mu_3\theta_3}\langle\mathbf{a}n'|V(\mathbf{r})|\mathbf{0}n\rangle, \tag{11}$$

and $H_n(\theta_3)$ is obtained from the expectation value H_n for the KE and a Bloch sum over coupling integrals for varying μ_3 and $\boldsymbol{\alpha}=\mathbf{0}$,

$$H_n(\theta_3)=H_n+\sum_{\mu_3} e^{i\mu_3\theta_3}\langle\mu_3\mathbf{a}_3n'|V(\mathbf{r})|\mathbf{0}n\rangle. \tag{12}$$

The secular problems (6) and (10), obtained for the two-dimensional and three-dimensional case, respectively, are equivalent, since $\delta(\theta_3'-\theta_3)$ separates (10) with respect to the field direction. The transition from the two-dimensional to the three-dimensional case is achieved by the replacement of the energy integral H_n and the coupling integrals $U_{n'n}(\boldsymbol{\alpha})$ by their Bloch sums $H_n(\theta_3)$ and $U_{n'n}(\boldsymbol{\alpha},\theta_3)$ with respect to the a_3 direction. Therefore, in the following sections we generally treat the two-dimensional case (6) and return to the three-dimensional case (10) only in order to obtain the correct electron-state density.

In applying (6) and (10) we have to keep in mind, firstly, that the separating δ functions $\delta_{n'n}$, $\delta_{\alpha'\alpha}$, $\delta(\theta_3'-\theta_3)$ multiplying the energy-term result from the omission of all overlap integrals; and, secondly, that the most important coupling integrals between orbitals at adjacent sites are not generally characterized by low values of μ_1 and μ_2, because of the choice of an arbitrary basis $\mathbf{a}_i$. Except for highly symmetric field directions, none of the nearest-neighbor coupling integrals can be found within the $U_{n'n}(\boldsymbol{\alpha})$, so that only the three-dimensional approach is meaningful.

III. NEARLY-FREE-ELECTRON METHOD

For the nearly-free-electron method we keep the condition $\mathbf{B}\|\mathbf{a}_3$ and introduce a Cartesian coordinate system, x, y, z, where the z direction coincides with $\mathbf{a}_3$, and, consequently, the xy plane coincides with the plane spanned by $\mathbf{b}_1$ and $\mathbf{b}_2$.

For the vector potential it is more appropriate to use instead of (2) the asymmetric gauge

$$\mathbf{A}(\mathbf{r})=B[0,x,0]. \tag{13}$$

With this gauge, the Schrödinger equation (2) takes the form

$$(H-E)\psi=\{-\tfrac{1}{2}\nabla_x^2+\tfrac{1}{2}(-i\nabla_y-Bx)^2-\tfrac{1}{2}\nabla_z^2 +V(\mathbf{r})-E\}\psi(\mathbf{r})=0. \tag{14}$$

For the lattice potential we use (following the nearly-free-electron method) the Fourier expansion

$$V(\mathbf{r})=\sum_{\mathbf{b}} V(\mathbf{b})e^{i\mathbf{b}\cdot\mathbf{r}}, \quad V(-\mathbf{b})=V^*(\mathbf{b}), \tag{15}$$

where $\mathbf{b}$ runs over all reciprocal lattice vectors; $\mathbf{b}=\sum_i \mu_i\mathbf{b}_i$. Splitting up $\mathbf{b}$ into the components

$$\mathfrak{b}=\mu_1\mathbf{b}_1+\mu_2\mathbf{b}_2, \quad \mathbf{b}=\mathfrak{b}+\mu_3\mathbf{b}_3, \tag{16}$$

we note that $\mathfrak{b}\cdot\mathbf{r}$ projects $\mathbf{r}$ on the xy plane [or $(\mathbf{b}_1,\mathbf{b}_2)$ plane], while z affects merely $\mathbf{b}_3\cdot\mathbf{r}$.

In order to separate the Hamiltonian (14) with respect to the field direction, we follow a procedure which is closely related to that applied in the tight-binding method. However, the roles of the real space and reciprocal lattices are interchanged. We distinguish once more between the two-dimensional approach, in which $V(\mathbf{r})$ shows no variation parallel to the field direction, and the more general three-dimensional approach.

In the former case we are left with

$$\{-\tfrac{1}{2}\nabla_x^2+\tfrac{1}{2}(-i\nabla_y-B_x)^2+\sum_{\mathfrak{b}} V(\mathfrak{b})e^{i\mathfrak{b}\cdot\mathbf{r}}-E\}\times\psi(x,y)=0. \tag{17}$$

The omission of all Fourier components $V(\mathbf{b})$ with $\mu_3\neq 0$ implies that, for most field directions, actually none of the most important Fourier components corresponding to nearest neighbors in the reciprocal lattice remains. An investigation of (17) then provides qualitative information on the level structure. For quantitative results, however, it is necessary to solve the three-dimensional secular problem. The treatment of the two-dimensional equation (17) can be shown to yield an already correct level structure, if $\mathbf{B}$ takes a highly symmetric lattice direction, so that most neighbors lie in the $(\mathbf{b}_1,\mathbf{b}_2)$ plane, and overlap regions distant from this plane can be excluded on energetic reasons.

Turning to the three-dimensional Schrödinger equation (14) we ignore in a first step the xy components of the KE and solve

$$\{-\tfrac{1}{2}\nabla_z^2+V(\mathbf{r})-E\}c(x,y;z)=0. \tag{18}$$

Equation (18) is an ordinary differential equation of second order with regard to the z variable. As potential we use the total lattice potential $V(\mathbf{r})$, which is periodic in z, with the period being $\mathbf{a}_3$ according to our choice of coordinates. The variables x, y normal to $\mathbf{B}$ are to be treated as external parameters. Thus, using Floquet's theorem, we classify the eigenstates of (18) by their wave number θ_3. We denote the eigenstates and eigenvalues by $c_{\theta_3}(x,y;z)$ and $E(x,y;\theta_3)$, respectively, with

$$c_{\theta_3}(x,y;z+a_3)=e^{i\theta_3}c_{\theta_3}(x,y;z) \tag{19}$$

and find the partial eigenvalues $E(x,y;\theta_3)$ to be periodic not only with respect to θ_3, but also with respect to x and y.

In order to prove the latter, we displace $\mathbf{r}$ in $V(\mathbf{r})$ by $(a_{ix},a_{iy},0)$, i.e., the xy component of $\mathbf{a}_i(i=1,2)$. This is equivalent to a displacement of z by the negative z component $-a_{iz}$, according to the general relation $V(\mathbf{r}+\mathbf{a}_i)=V(\mathbf{r})$. Such a change of z in the potential $V(\mathbf{r})$ of (18) does not affect the eigenvalues $E(x,y;\theta_3)$, but results in replacing $c_{\theta_3}(x,y;z)$ by $c_{\theta_3}(x,y;z-a_{iz})$.

Consequently, we can expand $E(x,y;\theta_3)$ into the Fourier series

$$E(x,y;\theta_3)=\sum_{\mathfrak{b}} V(\mathfrak{b},\theta_3)e^{i\mathfrak{b}\cdot\mathbf{r}}, \tag{20}$$

where the notation $V(\mathfrak{b},\theta_3)$ for the Fourier components is chosen so as to emphasize the fact that $E(x,y;\theta_3)$ serves as potential for the following integrations within the xy plane. $E(x,y;\theta_3)$ is independent of $\mathbf{B}$, since in (18) by cancelling the xy components of the KE we also cancelled the magnetic field.

Knowing the set $\{c_{\theta_3}(x,y;z)\}$ and $\{E(x,y;\theta_3)\}$ of eigenstates and eigenvalues of Eq. (18) we try to solve the Schrödinger equation (14) with the ansatz

$$\psi(\mathbf{r})=\sum_{\theta_3} c_{\theta_3}(x,y;z)\psi_{\theta_3}(x,y). \tag{21}$$

We can separate the equation with respect to θ_3, and we obtain

$$\{-\tfrac{1}{2}\nabla_x^2+\tfrac{1}{2}(-i\nabla_y-Bx)^2+E(x,y;\theta_3)-E\}\times\psi_{\theta_3}(x,y)=0, \tag{22}$$

if we assume that all spatial derivatives $\nabla V(\mathbf{r})$ of the lattice potential can be neglected, compared to $V(\mathbf{r})$ itself. Explicitly, we neglect $\nabla_{x,y}c_{\theta_3}(x,y;z)$ and $\nabla_{x,y}^2\times c_{\theta_3}(x,y;z)$ compared to $E(x,y;\theta_3)$ and $c_{\theta_3}(x,y;z)$.

The error linked with the separation (22) can be estimated, if we assume that the motion of wave packets in reciprocal space follows approximately the Lorentz equation. That is, we do not consider an interaction of states with different wave number θ_3. Substituting (21) into the Schrödinger equation (14), multiplying with $c_{\theta_3}^*(x,y;z)$ from the left, and integrating over z, we dispose of the hitherto arbitrary xy-dependent phase in $c_{\theta_3}(x,y;z)$ such that $\int dz\, c_{\theta_3}^*(x,y;z)\nabla_{x,y}c_{\theta_3}(x,y;z)=0$. We are left then with the second derivatives $\int dz\, c_{\theta_3}^*(x,y;z)\nabla_{x,y}^2c_{\theta_3}(x,y;z)$, which we include into the potential $E(x,y;\theta_3)$. After some transformations we find that

$$E_1(x,y;\theta_3)=-\tfrac{1}{2}\int dz\, c_{\theta_3}^*(x,y;z)(\nabla_x^2+\nabla_y^2)c_{\theta_3}(x,y;z)$$

$$=\tfrac{1}{2}\sum_{\mathbf{b}',\mathfrak{b},\mu_3'=\mu_3\neq 0}\frac{[\nabla_{x,y}V(\mathbf{b}')e^{i\mathbf{b}'\cdot\mathbf{r}}]^*\nabla_{x,y}V(\mathbf{b})e^{i\mathfrak{b}\cdot\mathbf{r}}}{[E(\theta_3+2\pi\mu_3)-E(\theta_3)]^2}, \tag{23}$$

with $\nabla_{x,y}$ being the two-dimensional ∇ operator $(\nabla_x,\nabla_y,0)$. The keeping of the spatial derivatives of $c_{\theta_3}(x,y;z)$ results in an extra potential $E_1(x,y;\theta_3)$ in (22). $E_1(x,y;\theta_3)$ can be considered small compared to

$E(x,y;\theta_3)$ if the Fourier components $V(\mathbf{b})$ with $\mu_3 \neq 0$ produce an only smoothly varying potential in the $(\mathbf{b}_1,\mathbf{b}_2)$ plane, i.e., if $\mathbf{B}$ takes a highly symmetric lattice direction. For other field directions (22) must be refined by adding the Lorentz potential $E_1(x,y;\theta_3)$. {Note that

$$\nabla_{x,y}u(\mathbf{r})\cdot\nabla_{x,y}v(\mathbf{r})=[\mathbf{B}\times\nabla u(\mathbf{r})]\cdot[\mathbf{B}\times\nabla v(\mathbf{r})]/B^2$$

with arbitrary functions $u(\mathbf{r})$, $v(\mathbf{r})$.}

Throughout this paper we generally think in terms of the simpler two-dimensional case (17), yet refer to the three-dimensional equations (18) and (22) for quantitative reasons. The essential change between both cases is achieved by replacing $V(\mathfrak{k})$ with $V(\mathfrak{k},\theta_3)$.

IV. ONE-DIMENSIONAL POTENTIALS

For a perturbation treatment of (17) [or (22)] we note that in the limit of vanishing lattice potential it can be separated by applying Floquet's theorem in the y direction. Substituting

$$\psi=e^{ik_y}\varphi(x), \tag{24}$$

we are left with a harmonic-oscillator equation in the x direction, whose eigenvalues are the equidistant Landau levels

$$E=B(n+\tfrac{1}{2}), \tag{25}$$

and whose eigenfunctions are the Hermite functions

$$h_n\left(x-\frac{k_y}{B}\right)=\left(\frac{1}{2^n n!}\sqrt{\frac{B}{\pi}}\right)^{1/2}H_n(\xi)e^{-\xi^2/2};\qquad \xi=(\sqrt{B})x-k_y/B. \tag{26}$$

Then, calculating the matrix elements of the lattice potential with respect to the free-electron functions (24), we obtain

$$\langle\psi'|\,V(\mathbf{r})\,|\psi\rangle=\sum_{\mathfrak{k}}V(\mathfrak{k})\delta(k_y'-k_y-\beta_y)\langle\varphi'|\,e^{i\beta_x x}\,|\varphi\rangle. \tag{27}$$

The δ function $\delta(k_y'-k_y-\beta_y)$ in (27) means that only those oscillator functions interact, whose origins are separated by $\Delta x=\beta_y/B$. Thus the system of functions to be used in a perturbation treatment of (17) is reduced to functions of the form

$$e^{i(k_y+\beta_y)y}h_n[x-(k_y+\beta_y)/B]. \tag{28}$$

The selection rule $\Delta x=\beta_y/B$ for the origin of interacting states is the basis for Pippard's[7,8] investigations of magnetic breakdown and the Landau level broadening by means of the orbit lattice. We use the orbit lattice throughout this paper repeatedly as a very useful interpretation, although our calculations are not based on it at any stage. For more information on the orbit lattice, we refer the reader to Pippard's original papers.

We return to the general treatment of two-dimensional lattice potentials normal by $\mathbf{B}$ by means of functions analogous to (28) in the next section. In this section we temporarily assume $V(\mathbf{r})$ to be independent of $\mathbf{b}_2\cdot\mathbf{r}$. (Note the simultaneous use of two different coordinate systems. We do not assume x,y to coincide with $r_1=\mathbf{b}_1\cdot\mathbf{r}/b_1$, $r_2=\mathbf{b}_2\cdot\mathbf{r}/b_2$.) To solve the Schrödinger equation (17) with the remaining one-dimensional potential we make the ansatz

$$\psi=\sum_{\beta\|\mathbf{b}_1}e^{i(k_y+\beta_y)y}\chi_\beta[x-(k_y+\beta_y)/B], \tag{29}$$

where the $\chi_\beta(x)$ are an arbitrary set of functions. By inserting (29) into (17), eliminating the y dependence by a Fourier transform, and shifting the origin of x to $(k_y+\beta_y)/B$, we obtain

$$\{-\tfrac{1}{2}\nabla_x^2+\tfrac{1}{2}(Bx)^2-E\}\chi_\beta(x)+\sum_{\beta'\|\mathbf{b}_1}V(\mathfrak{k}')\times\exp\left[i\beta_x'\left(x+\frac{k_y+\beta_y}{B}\right)\right]\chi_{\beta-\beta'}\left(x+\frac{\beta_y'}{B}\right)=0. \tag{30}$$

The only term depending explicity on $\mathfrak{k}$ is the phase factor $\exp(i\beta_x\beta_y/B)$ in the perturbing term. This exponential, as well as the wave number k_y, can be eliminated by the substitution

$$\chi_\beta(x)=\exp\left[i\left(\frac{\beta_x k_y}{B}+\frac{\beta_x\beta_y}{2B}\right)\right]\chi(x). \tag{31}$$

We are then left with the single equation

$$\{-\tfrac{1}{2}\nabla_x^2+\tfrac{1}{2}(Bx)^2-E\}\chi(x)+\sum_{\beta\|\mathbf{b}_1}V(\mathfrak{k})\exp\left[i\beta_x\left(x+\frac{\beta_y}{2B}\right)\right]\chi\left(x+\frac{\beta_y}{B}\right)=0. \tag{32}$$

The eigenfunctions of (32) for vanishing lattice potential are once more the Hermite functions $h_n(x)$ as given by (26). For the matrix elements of $\exp[i\beta_x(x+\beta_y/2B)]$ with respect to $h_n(x)$ we find, following a procedure similar to that of Quinn and Rodriguez,[11] that

$$c_{n'n}(\mathfrak{k})=\left\langle h_{n'}(x)\left|\exp\left[i\beta_x\left(x+\frac{\beta_y}{2B}\right)\right]\right|h_n\left(x+\frac{\beta_y}{B}\right)\right\rangle=\exp\left(-\frac{\beta^2}{4B}\right)\left(\frac{n!n'!}{2^{n+n'}}\right)^{1/2}\sum_\sigma\frac{2^\sigma}{(n'-\sigma)!(n-\sigma)!\sigma!}\times\left(\frac{\beta_x+i\beta_y}{i\sqrt{B}}\right)^{n'-\sigma}\left(\frac{\beta_x-i\beta_y}{i\sqrt{B}}\right)^{n-\sigma}, \tag{33}$$

where the sum over σ can be replaced by Laguerre

[11] J. J. Quinn and S. Rodriguez, Phys. Rev. **128**, 2487 (1962).

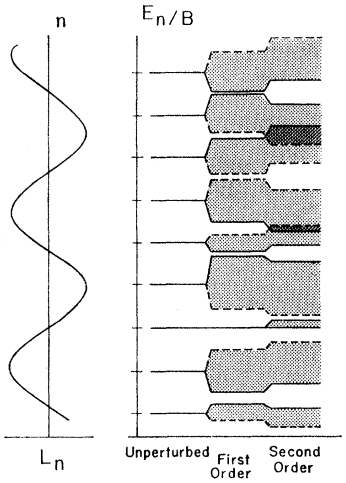

FIG. 1. Broadening and shift of Landau levels in a one-dimensional lattice. Solid lines, $V(\mathbf{b}_1)$ positive real; dashed lines, $V(\mathbf{b}_1)$, negative real.

polynomials, yielding

$$c_{n'n}(\boldsymbol{\beta})=\exp\left(-\frac{\beta^2}{4B}\right)\left(\frac{2^n n!}{2^{n'}n'!}\right)^{1/2}\left(\frac{\beta_x+i\beta_y}{i\sqrt{B}}\right)^{n'-n}\times L_n{}^{n'-n}\left(\frac{\beta^2}{2B}\right). \quad (34)$$

Thus, from a perturbation treatment of (32) up to second order in $V(\boldsymbol{\beta})$, we obtain

$$E_n=B(n+\tfrac{1}{2})+\sum_{\boldsymbol{\beta}\|\mathbf{b}_1} V(\boldsymbol{\beta})\exp\left(-\frac{\beta^2}{4B}\right)L_n\left(\frac{\beta^2}{2B}\right)+E_n{}^{(2)}, \quad (35)$$

$$E_n{}^{(2)}=\sum_{n'\neq n}\frac{n!/n'!}{B(n-n')}\left(\frac{\beta^2}{2B}\right)^{n'-n}\times\left|\sum_{\boldsymbol{\beta}\|\mathbf{b}_1} V(\boldsymbol{\beta})\exp\left(-\frac{\beta^2}{4B}\right)L_n{}^{n'-n}\left(\frac{\beta^2}{2B}\right)\right|^2. \quad (36)$$

The zeroth-order term yields equidistant Landau levels. The first-order term was discussed by Reitz[12] in his investigations of the magnetic breakdown probability. Using asymptotic expansions for the Laguerre polynomials,[13] one finds that $\exp[-\beta^2/4B]$ dominates $L_n{}^{n'-n}(\beta^2/2B)$ for $(\frac{1}{2}\beta)^2>B(n'+n+1)\approx E_{n'}+E_n$, that is, as long as there is no sizable overlap between the unperturbed orbitals $h_n(x)$. Their extension increases approximately as $\sqrt{E_n}$; the region of overlap, therefore, is reached for $E_{n'}+E_n\approx B(n'+n+1)>(\frac{1}{2}\beta)^2$, where $\exp[-\beta^2/4B]L_n{}^{n'-n}(\beta^2/2B)$ is found to oscillate with an amplitude proportional to $(n'+n+1)^{-1/2}$. The maximum shift of Landau levels due to the first-order terms in $V(\boldsymbol{\beta})$ is obtained when the diameter of the corresponding orbit in k space just touches the Brillouin-zone boundaries.

While considering shifts of the Landau levels, we have not yet taken into account the relative position of the gauge center $x,y=0$ and the lattice potential $V(\mathbf{r})$. The fixing of the gauge center and the shifting of the origin of the lattice potential $V(\mathbf{r})$ to $\mathbf{r}_0$ can be taken into account by the replacement of $V(\mathbf{b})$ by $V(\mathbf{b})\exp(i\mathbf{b}\mathbf{r}_0)$, i.e.,

$$V(\mathbf{b})\xrightarrow[\mathbf{r}+\mathbf{r}_0]{} V(\mathbf{b})e^{i\mathbf{b}\cdot\mathbf{r}_0}. \quad (37)$$

Thus the eigenvalue equations (35) and (36) yield not only a shift of Landau levels, but also a broadening of these levels into narrow bands.

The effect of the terms of second order in $V(\boldsymbol{\beta})$ on E_n in general is similar to that of the first-order terms. They become important especially near the zeros of $L_n(\beta^2/2B)$, by causing the level broadening not to vanish completely. To find the mutual shift of neighboring Landau levels due to the second-order terms, we restrict ourselves to the leading terms $n'=n\pm1$, $\boldsymbol{\beta}=\pm\mathbf{b}_1$. Then, using some standard recursion formulas for Laguerre polynomials we find that

$$E_n=B(n+\tfrac{1}{2})+[V(\mathbf{b}_1)+V^*(\mathbf{b}_1)]e^{-b_1^2/4B}\times L_n(b_1^2/2B)+E_n{}^{(2)}, \quad (38)$$

$$E_n{}^{(2)}=(1/B)[V(\mathbf{b}_1)+V^*(\mathbf{b}_1)]^2e^{-b_1^2/2B}[(L_{n+1}-L_{n-1})L_n+(2B/b_1^2)(L_{n+1}-L_n)(L_n-L_{n-1})]. \quad (39)$$

The mutual repulsion of neighboring levels by the second-order terms turns out to be strictly correlated to their broadening by the first-order terms. In general, the levels are pushed towards the energy direction with increasing level broadening.

Figure 1 shows a section of the resulting level system near the Fermi energy, which we assumed $E_F=\frac{1}{6}b_1^2$, so that the corresponding quasiclassical orbits in k space cross the Brillouin-zone boundaries $\pm\frac{1}{2}b_1$ with an angle of about 30°. For the Laguerre polynomials we use an asymptotic formula for fixed argument[13]

$$\exp\left(-\frac{b_1^2}{4B}\right)L_n\left(\frac{b_1^2}{2B}\right)=\frac{\cos[2((n+\frac{1}{2})b_1^2/2B)^{1/2}-\frac{1}{4}\pi]}{\pi^{1/2}((n+\frac{1}{2})b_1^2/2B)^{1/4}}. \quad (40)$$

The phase of the cosine in (40) strongly depends on B; however, the phase difference between $L_{n'}$ and L_n is just $(n'-n)[b_1^2/2B(n+\frac{1}{2})]^{1/2}$. The band edges due to relative displacements (37) of the gauge center and the lattice potential generally are obtained by replacing $V(\mathbf{b}_1)$ by $|V(\mathbf{b}_1)|$ and $-|V(\mathbf{b}_1)|$, respectively. We have distinguished these cases in Fig. 1 by solid and dashed lines. Different edges may overlap, since the corresponding differential equations (32) are not coupled. An ex-

[12] J. R. Reitz, J. Phys. Chem. Solids **25**, 53 (1964).
[13] *Higher Transcendental Functions*, edited by A. Erdelyi (McGraw-Hill Book Co., New York, 1953), Vol. 2, p. 199.

ception are the zeros $L_n(b_1^2/2B)=0$. The level broadening in this case is due to the second-order terms and the band edges are obtained by replacing $V(\mathbf{b}_1)$ by $|V(\mathbf{b}_1)|$ and $i|V(\mathbf{b}_1)|$, respectively.

Variations of the magnetic field change the phase of the cosine term in (40), thus shifting either up or down the approximate curve for L_n shown in the left-hand diagram of Fig. 1. This causes rapid simultaneous changes of the bandwidths and the mutual repulsion shown in the right-hand diagram of Fig. 1.

V. TWO-DIMENSIONAL POTENTIALS

In Sec. IV we were able to separate the one-dimensional set of differential equations (30) for $\chi_\beta(\beta\|\mathbf{b}_1)$ by introducing an appropriate phase factor. We obtained an uncoupled set of equations (32), whose eigenvalues may be degenerate.

Turning back now to two-dimensional lattice potentials, we find that an analogous separation no longer is generally possible, since in deriving (32) we explicitly used $\exp[i(\beta'\times\beta)_z/2B]=1$ for all reciprocal lattice vectors β, β' under consideration, $(\beta,\beta'\|\mathbf{b}_1)$. However, also for a two-dimensional variety of vectors β, β' there are similar possibilities for separating (30) with respect to β. That is, $\exp[i(\beta'\times\beta)_z/2B]$ becomes equal to 1, if we assume $(\beta'\times\beta)_z/2B$ to be an integer multiple of 2π for all combinations β, β', which obviously is true if required for the basis vectors $\mathbf{b}_1$, $\mathbf{b}_2$. Thus finding (32) to be valid again, but for all vectors $\beta\perp\mathbf{B}$, we apply the same perturbation treatment as in the one-dimensional case and obtain equations similar to (35) and (36), yet without the restriction $\beta\|\mathbf{b}_1$. The level structure shown in Fig. 1 is qualitatively maintained, except for the increased number of broadening Fourier components $V(\beta)$.

The condition used here, $(\mathbf{b}_1\times\mathbf{b}_2)_z/2B=2\pi M$, can be transformed by means of (3) to give $\mathbf{B}(\mathbf{a}_1\times\mathbf{a}_2)=2\pi/2M$. The magnetic flux ϕ per unit cell of the real lattice,

$$\phi=\mathbf{B}(\mathbf{a}_1\times\mathbf{a}_2), \tag{41}$$

has to be equal to 2π divided by an even integer, which is just the case Pippard discussed in his investigations on magnetic breakdown.[7,8] His procedure corresponds to a solution of Eq. (32) by means of $p\chi^{(1)}(x)+q\chi^{(2)}(x)$, where $\chi^{(1)}(x)$ and $\chi^{(2)}(x)$ describe different possible electron orbits in k space, and p, q are adjustable switching parameters ($p^2+q^2=1$). For $p=1$ one obtains Landau levels matching the area enclosed by the orbit corresponding to $\chi^{(1)}(x)$; for $q=1$ one obtains Landau levels matching the area enclosed by the orbit corresponding to $\chi^{(2)}(x)$. The level broadening given by (35) corresponds to that obtained by Pippard near these limiting cases $p=1$ and $q=1$, i.e., the dependence of p and q on B may be taken from (35) and (40).

The condition of rational fluxes per unit cell, $\mathbf{B}(\mathbf{a}_1\times\mathbf{a}_2)=2\pi/M$, has been used repeatedly in derivations of one-dimensional effective Hamiltonians. Among these we mention the reciprocal methods of Harper[2] and of Zak.[10] Harper uses the $E(\hat{k})$ operator introduced by Peierls,[1] which he separates by means of plane waves in the y direction and arbitrary functions in the x direction. Approximating the latter functions by the WKB method he ignores the translational properties imposed on the eigenfunctions by the magnetic field. He obtains the correct broadening but no splitting of the Landau levels. Zak, on the other hand, uses functions adapted *a priori* to the magnetic translation group.[14,15] He reduces the two-dimensional Hamiltonian by means of the relations imposed on the Fourier components of these adapted functions by the periodic boundary conditions. This group theoretical procedure yields necessarily the correct information on the magnetic band splitting. The method applied in the present paper is a generalization of that given in Ref. 4. The derivation of (32) inclusive of the two-dimensional extension to $\beta\perp\mathbf{B}$, follows the procedure of Harper, i.e., the Hamiltonian is separated without regard to the magnetic translation group. Compatibility with the latter is obtained in Sec. IV by using Landau orbitals in each stage of the perturbation treatment, and in the following sections by applying periodic boundary conditions.

Going back to arbitrary values of the flux ϕ, we find the set of differential equations (30) to split up into $2N$ subsets, whenever ϕ equals $2\pi M/N$. This gives rise to a splitting of each broadened Landau level into N subbands.

In order to treat the two-dimensional nearly-free-electron approach in a completely general fashion and to show its close relations to the tight-binding approach we now introduce the perturbation treatment mentioned in Sec. IV. We use a set of ansatz functions similar to those defined in (28), namely,

$$|\beta n\rangle=\exp[i(k_y+\beta_y)y]\exp[i(k_y+\tfrac{1}{2}\beta_y)\beta_x/B]\times\varphi_n[x-(k_y+\beta_y)/B]. \tag{42}$$

The second exponential on the right-hand side is included so as to follow as close as possible the procedure used for the one-dimensional case. In (42) we use general functions $\varphi_n(x)$ instead of the Hermite functions $h_n(x)$; this enables us to include orthogonal orbitals already corresponding to a given nearly-free-electron band structure, although we mostly think in terms of Hermite functions $h_n(x)$. The calculation of the matrix elements of the Hamiltonian (17) with $|\beta n\rangle$ yields

$$\langle\beta' n'|H-E|\beta n\rangle=(H_n-E)\delta_{n'n}\delta_{\beta'\beta}+C_{n'n}(\beta'-\beta)\times V(\beta'-\beta)\exp[i(\beta'\times\beta)_z/2B], \tag{43}$$

where H_n, as in the tight-binding case, is an expectation value for the KE

$$H_n=\langle\varphi_n(x)|\tfrac{1}{2}[-i\nabla-\mathbf{A}(\mathbf{r})]^2|\varphi_n(x)\rangle \tag{44}$$

[14] E. Brown, Phys. Rev. **133**, A1038 (1964).
[15] J. Zak, Phys. Rev. **134**, A1602 (1964).

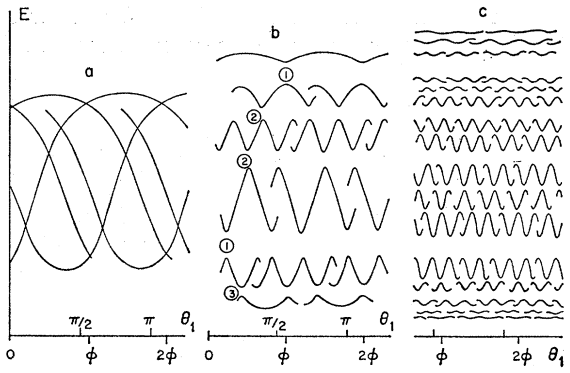

FIG. 2. Graphic perturbation treatment: (a) unperturbed bands, (b) splitting of intersections up to third order, and (c) splitting of intersections up to ninth order.

and $C_{n'n}(\beta)$, in close analogy to (33), is given by

$$C_{n'n}(\beta) = \langle \varphi_{n'}(x) | \exp[i\beta_x(x+\beta_y/2B)] | \varphi_n(x\times\beta_y/B)\rangle. \quad (45)$$

In deriving (43) we assumed that the set of basis functions (42) is independent, i.e., that no two vectors β have the same value of β_y. This implies that the two coordinate systems x,y and $\mathbf{r}_1,\mathbf{r}_2$ are not commensurate. Recalling that the system x,y is fixed by the choice of the vector potential, while r_1,r_2 correspond to the basis vectors of the lattice, we have avoided any simultaneous period of the ansatz functions $|\beta n\rangle$ with respect to the y direction. Each such period entails a field-dependent selection rule for the origins of $\varphi_n(x)$, thus requiring a separate treatment of rational and irrational fluxes $\phi/2\pi$ at a too early stage. We need rational fluxes in fact only for quantitative numerical reasons.

Equation (43) has exactly the same form as the central equation (6) for the tight-binding approach. The energy integrals H_n between atomic orbitals in the real lattice are replaced by energy integrals H_n between Landau orbitals in the orbit lattice. The coupling integrals between atomic orbitals in the real lattice in like manner are replaced by coupling integrals between Landau orbitals in the orbit lattice. The band index of the atomic orbitals has become the quantum number for the Landau levels.

Comparing the exponentials in (6) and (43) we find that they yield just opposite phase shifts. The center of the magnetic orbit $|\beta n\rangle$ in real space is given by

$$\sigma = (\beta_y/B, -\beta_x/B, 0), \quad (46)$$

so that the exponential in (40) can be rewritten to give

$$\exp[i(\beta'\times\beta)_z/2B] = \exp[\tfrac{1}{2}\mathbf{B}\cdot(\sigma'\times\sigma)]. \quad (47)$$

The phase shift on a transition from $|\beta n\rangle$ to $|\beta' n'\rangle$ equals the negative flux through the parallelogram spanned by σ and σ'. The reason for this opposite sign compared to the tight-binding result (6) is as follows: A switch by a vector α of the real lattice maintains the lattice potential and changes the gauge of the electron orbits. On the other hand, a switch by a vector σ of the orbit lattice maintains the gauge of the electron orbit but changes its position relative to the lattice potential. This can be compensated by a shift of the lattice potential in the opposite direction.

Compensating for this opposite phase shift by transposing the secular determinant for the orbit lattice, we note the following equivalences:

$$|\alpha n\rangle \leftrightarrow \langle \beta n|, \quad \mathbf{B}(\alpha\times\alpha') \leftrightarrow (\beta'\times\beta)_z/B,$$
$$H_n \leftrightarrow H_n, \quad U_{n'n}(\alpha) \leftrightarrow [C_{n'n}(\beta)V(\beta)]^*. \quad (48)$$

In general, we use the notation of the tight-binding method, but repeatedly take into account the much stronger field dependence of the integrals which appear in the nearly-free-electron theory.

The equivalences given in (48) can be extended successfully also to the three-dimensional case. If for the three-dimensional extension of the basis functions (42) we use $|\beta\theta_3 n\rangle = c_{\theta_3}(x,y;z)|\beta n\rangle$, we find (48) to hold with H_n, $U_{n',n}(\alpha)$, $V(\beta)$ replaced by $H_n(\theta_3)$, $U_{n',n}(\alpha,\theta_3)$, $V(\beta,\theta_3)$, respectively.

VI. ONE-DIMENSIONAL SECULAR PROBLEM

In order to separate the two-dimensional matrix (6) or (43) we follow closely the procedure introduced in an earlier paper on the tight-binding approach to finite crystals[4]; that is, we transform $|\alpha n\rangle$ according to

$$|\theta_1\mu_2 n\rangle = \sum_{\mu_1} \exp[-i\mu_1(\theta_1 - \tfrac{1}{2}\mu_2\phi)]|\alpha n\rangle. \quad (49)$$

Equation (49) is a Bloch sum for the α_1 direction, yet with the wave number θ_1 modified by $\frac{1}{2}\mu_2\phi$. The matrix elements of $H-E$ with respect to (49) are

$$\langle \theta_1'\mu_2' n'|H-E|\theta_1\mu_2 n\rangle = \delta(\theta_1'-\theta_1)\{(H_n-E)\delta_{n'n}\delta_{\mu_2'\mu_2} + \sum_{\mu_1'-\mu_1} \exp[i(\mu_1'-\mu_1)(\theta_1 - \tfrac{1}{2}(\mu_2'+\mu_2)\phi)] \times U_{n'n}(\alpha'-\alpha)\}, \quad (50)$$

where we have made use of (6). In this and in the following section we assume the coupling integrals $U_{n'n}(\alpha)$ to vanish for $n'\neq n$ (one-band approach), so that we are left with a one-dimensional secular problem. A one-band approximation certainly is more in accord with the tight-binding than with the nearly-free-electron method. The former method, in fact, turns out to include the low-field, as well as the high-field case. In the nearly-free-electron method the one-band approach corresponds to first-order perturbation theory; a perturbation treatment for degenerate states (such as the unperturbed Landau orbitals for fixed n) requires in first order their diagonalization with respect to the perturbing potential. Interactions between nondegenerate states (such as the Landau orbitals for $n'\neq n$) then cause second-order perturbation terms. We discuss these interband interactions qualitatively in Sec. VIII.

For a further simplification of our notation in the one-band case we put $E=H_n+E_n$ and $U_{nn}(\boldsymbol{\alpha})=U(\mu_1\mu_2)$. The secular determinant corresponding to (50) then becomes

$$\begin{vmatrix} \cdots\sum_{\mu_1}\exp[i\mu_1(\theta_1-(\mu-\frac{1}{2})\phi)]\,U(\mu_1 1) & & \\ \sum_{\mu_1}\exp[i\mu_1(\theta_1-\mu\phi)]\,U(\mu_1 2) & \cdots & \\ \cdots\sum_{\mu_1}\exp[i\mu_1(\theta_1-\mu\phi)]\,U(\mu_1 0)-E_n & & \\ \sum_{\mu_1}\exp[i\mu_1\theta(_1-(\mu+\frac{1}{2})\phi)]\,U(\mu_1 1) & \cdots & \\ \cdots\sum_{\mu_1}\exp[i\mu_1(\theta_1-(\mu+\frac{1}{2})\phi)]\,U(\mu_1 1) & & =0. \\ \sum_{\mu_1}\exp[i\mu_1(\theta_1-(\mu+1)\phi)]\,U(\mu_1 0)-E_n\cdots & & \\ \cdots\sum_{\mu_1}\exp[i\mu_1(\theta_1-(\mu+1)\phi)]\,U(\mu_1\bar{2}) & & \\ \sum_{\mu_1}\exp[i\mu_1(\theta_1-(\mu+\frac{3}{2})\phi)]U(\mu_1\bar{1}) & \cdots & \\ \cdots \quad \cdots & \cdots & \end{vmatrix} \quad (51)$$

For one-dimensional potentials in the $\mathbf{a}_1$ direction the determinant (51) is diagonal. This yields the level broadening shown in Fig. 1 (in first-order perturbation). Switching on the potential in the $\mathbf{a}_2$ direction gradually, first the nearest-neighbor coupling integrals and successively further off-diagonal terms have to be taken into account. The bands thus split into several subbands. Since a general perturbation treatment of (51) yields lengthy formulas, we illustrate the result to be expected in Fig. 2. Explicit calculations for fields parallel to a tetragonal or a hexagonal lattice axis are given in the next section. Figure 2(a) shows a portion of the one-dimensional energy bands given by the diagonal elements of (51). Neighboring diagonal elements are shifted in the θ_1 axis by an amount ϕ. In order to include all first-order interactions (with regard to the two-dimensional case), we plot each band over slightly more than one period, so that adjacent bands have just one period 2π in common. Figure 2(b) shows the energy bands which result from splitting all intersections when the off-diagonal elements of (51) are taken into account. In this way two gaps of first and second order and one gap of third order arise. They are distinguished by a decreasing gap width (and the indices 1, 2, 3). (In the three-dimensional case the nearest-neighbor coupling integrals may correspond to rather high values of μ_2, so that first-order intersections between more distant diagonal elements result.) The price we have to pay for limiting the extension of the one-dimensional bands is that the resulting bands still are limited fragments. Consequently in Fig. 2(c) we extended the one-dimensional bands over two more periods [extending in fact the bands obtained in Fig. 2(b)]. Now gaps up to ninth order occur. The gap width again is assumed to decrease with increasing order. Continuing this procedure until either the splitting becomes negligible or the bands happen to coincide (which requires rational fluxes, $\phi/2\pi=N/M$), we end up with a generally large number of field-dependent subbands, which evolve regularly into groups produced by the lowest-order gaps.

The secular determinant (51) and the perturbation treatment attached to it seem rather asymmetric with regard to the crystal directions $\mathbf{a}_1$, $\mathbf{a}_2$, The one-dimensional bands are produced by the integrals $U(\mu_1 0)$ and split up owing to the effects of $U(\mu_1\mu_2)$ with $\mu_2>0$. However, carrying out a perturbation treatment for a finite subdeterminant of order M, we find the symmetry with regard to $\mathbf{a}_1$, $\mathbf{a}_2$ restored as soon as M includes several periods ($M\phi\gg 2\pi$). The corresponding secular polynomial is conveniently obtained by the diagram technique described in Ref. 4, with the adjoined products given by (6). The diagram between any two positions $\boldsymbol{\alpha}$, $\boldsymbol{\alpha}'$ represents the interaction of the respective orbitals $|\boldsymbol{\alpha}n\rangle$, $|\boldsymbol{\alpha}'n\rangle$, thus contributing the factor $U(\boldsymbol{\alpha}'-\boldsymbol{\alpha})\exp[\frac{1}{2}i\mathbf{B}(\boldsymbol{\alpha}\times\boldsymbol{\alpha}')]$. Summing over all nonequivalent closed graphs which contain an equal number of diagrams, we obtain for the leading terms of the secular polynomial

$$E_n{}^M-ME_n{}^{M-2}\tfrac{1}{2}\sum_{\alpha+\alpha'=0}U(\boldsymbol{\alpha})U(\boldsymbol{\alpha}')$$

$$-ME_n{}^{M-3}\tfrac{1}{3}\sum_{\alpha+\alpha'+\alpha''=0}U(\boldsymbol{\alpha})U(\boldsymbol{\alpha}')U(\boldsymbol{\alpha}'')\exp[\tfrac{1}{2}iB(\boldsymbol{\alpha}\times\boldsymbol{\alpha}')]$$

$$+\cdots=0. \quad (52)$$

VII. TETRAGONAL AND HEXAGONAL AXES

In discussing the eigenvalues of (51) we noted a smooth transition between the level schemes for rational and irrational fluxes ϕ. Therefore, it is only a mild restriction to assume $\phi=2\pi N/M$ in the following investigations. Since the matrix elements of the secular problem (50) are periodic in $\frac{1}{2}(\mu_2+\mu_2')$ with period M, we apply Floquet's theorem to the eigenvectors. Then, using $\exp(iM\theta_2)$ as a separation parameter, we end up with a finite secular determinant, which results from (51) by limiting μ to $1\leq\mu\leq M$ and replacing $U(\mu_1\mu_2)$ by $\sum_\lambda U(\mu_1\mu_2+\lambda M)\exp[i\lambda M(\theta_2-\frac{1}{2}\mu_1\phi)]$. From a proper permutation of rows and columns one finds that its period with respect to θ_1 is also reduced to $2\pi/M$.

In order to obtain explicit energy bands we now make a nearest-neighbor approximation. To include directions with tetragonal, as well as with hexagonal lattice symmetry, we keep merely the coupling integrals

$$U(10),\ U(01),\ U(\bar{1}\bar{1})\neq 0 \quad (53)$$

[and their complex conjugates $U(\bar{1}0)$, $U(0\bar{1})$, $U(11)$]. We are left then with a much simplified secular determinant, which contains elements different from zero only on the diagonal, in the near diagonals, and in the upper-right and lower-left corners. Denoting its elements

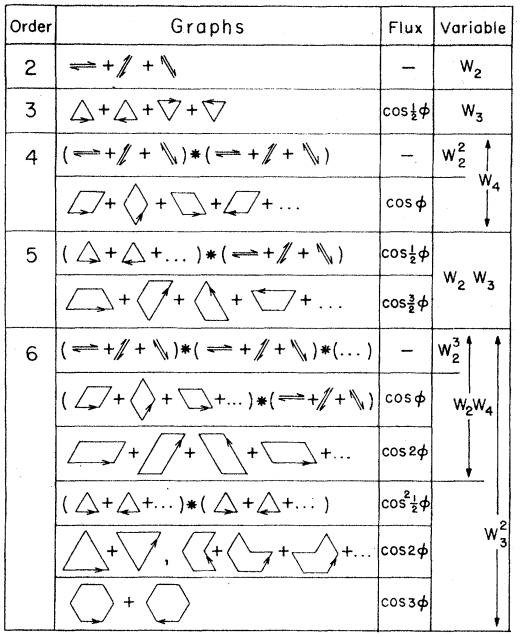

FIG. 3. Graphs contributing to a sixth-order perturbation treatment. Each single line indicates a transition between adjacent lattice sites; the corresponding matrix elements are given by Eqs. (6) and (43).

by $\det(\mu,\nu)$, we have

$$\det(\mu,\mu)=U(10)\ \exp[i(\theta_1-\mu\phi)]+U(\bar{1}0)\times\exp[-i(\theta_1-\mu\phi)]-E_n,$$

$$\det(\mu,\mu+1)=\det^*(\mu+1,\mu)=U(01)+U(11)\times\exp[i(\theta_1-(\mu+\tfrac{1}{2})\phi)],$$

$$\det(M,1)=\det^*(1,M)=\{U(01)+U(11)\times\exp[i(\theta_1-(M+\tfrac{1}{2})\phi)]\}\times\exp[iM\theta_2]. \quad (54)$$

Expanding this secular determinant in terms of products of its elements we know from its periodicity $2\pi/M$ with respect to ϕ that all nonconstant terms containing less than M factors $\exp(i\theta_1)$ cancel. The only terms dependent on θ_1, θ_2 are

$$W(\theta_1,\theta_2)=(-1)^{(M+1)N}[U(10)^M\exp(iM\theta_1)+\text{c.c.}]+(-1)^{M+1}[U(01)^M\exp(iM\theta_2)+\text{c.c.}]+(-1)^{M(N+1)+1}[U(11)^M\exp(iM(\theta_1+\theta_2))+\text{c.c.}]. \quad (55)$$

$W(\theta_1,\theta_2)$ clearly has the form of the nearest-neighbor tight-binding energy expression in tetragonal or hexagonal lattices. In our investigations, $U(10)$, $U(01)$, and $U(\bar{1}\bar{1})$ cannot be assumed to be *a priori* real. They may contain phase factors due to the relative shift of the gauge center and the lattice potential [as in (37)] or due to the phase shift at a switching point [as in (34)].

The constant part of the secular determinant can be conveniently expressed using the symmetric variables

$$W_2=|U(10)|^2+|U(01)|^2+|U(\bar{1}\bar{1})|^2,$$
$$W_3=\mathrm{Re}\{U(10)U(01)U(\bar{1}\bar{1})\}, \quad (56)$$
$$W_4=|U(10)U(01)|^2+|U(01)U(\bar{1}\bar{1})|^2+|U(\bar{1}\bar{1})U(10)|^2.$$

Summing over the graphs shown in Fig. 3 and the equivalent rotated and inverted graphs we obtain

$$\begin{aligned}E_n{}^M&-ME_n{}^{M-2}W_2+[M(M-3)/2!]E_n{}^{M-4}W_2{}^2\\&-[M(M-4)(M-5)/3!]E_n{}^{M-6}W_2{}^3\pm\cdots\\&-ME_n{}^{M-3}4\cos\tfrac{1}{2}\phi W_3+M[(M-3)/1!\\&-\sin\tfrac{3}{2}\phi/\sin\tfrac{1}{2}\phi]E_n{}^{M-5}4\cos\tfrac{1}{2}\phi W_2W_3\mp\cdots\\&-M(\sin\tfrac{3}{2}\phi/\sin\tfrac{1}{2}\phi)E_n{}^{M-4}W_4\\&+M[(M-5)\sin\tfrac{3}{2}\phi/1!\sin\tfrac{1}{2}\phi\\&-\sin\tfrac{5}{2}\phi/\sin\tfrac{1}{2}\phi]E_n{}^{M-6}W_2W_4\mp\cdots\\&+M[2(1+\sin\tfrac{3}{2}\phi/\sin\tfrac{1}{2}\phi)(M-5)/1!\\&-(3+\sin\tfrac{3}{2}\phi/\sin\tfrac{1}{2}\phi)\\&\times\sin\tfrac{5}{2}\phi/\sin\tfrac{1}{2}\phi]E_n{}^{M-6}W_3{}^2\mp\cdots\\&+(-1)^MW(\theta_1,\theta_2)=0, \quad (57)\end{aligned}$$

where $\phi=2\pi N/M$. Equation (57) generally yields M allowed subbands for E_n, with the band edges corresponding to the extremal values of $W(\theta_1,\theta_2)$.

We begin our discussion of this level scheme with the case $U(10)\neq 0$, $U(01)=U(\bar{1}\bar{1})=0$, then gradually increase $U(01)$ to $U(01)=U(10)$, and finally increase $U(\bar{1}\bar{1})$ to $U(10)=U(01)=U(\bar{1}\bar{1})$. Thus we systematically evolve from a one-dimensional lattice to a tetragonal structure and from this to hexagonal lattice; the intermediate values correspond to orthorhombic and monoclinic structures.

Putting $U(01)=U(\bar{1}\bar{1})=0$ entails that also W_3 and W_4 vanish. The eigenvalue equation (57) becomes a Tchebichef polynomial of order M in $E_n/2\sqrt{W_2}$. The energies corresponding to the extremal values

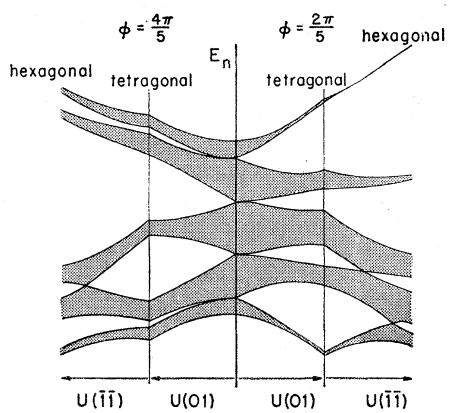

FIG. 4. Magnetic subbands for $M=5$ and a gradual evolution of the tetragonal and hexagonal symmetry.

$\pm 2|U(10)|^M$ of $W(\theta_1,\theta_2)$ are

$$E_n=2|U(10)|\cos(\lambda\pi/M) \quad (\lambda=0,1,\cdots,M). \quad (58)$$

The one-dimensional bands are not yet split, but (58) denotes the energies, where the splitting for $U(01)$ $\ll U(10)$ begins.

Going to arbitrary values of $U(10)$ [with $U(\bar{1}\bar{1})$ still equal to zero] we note that in (57) either even or odd powers of E_n occur. The level splitting thus is symmetric with respect to the center $E_n=0$. The extremal values of $W(\theta_1,\theta_2)$ are given by

$$W(\theta_1,\theta_2)_{ex}=\pm 2[|U(10)|^M+|U(01)|^M]. \quad (59)$$

Due to additional symmetries of the secular determinant (54) at these band edges (the eigenvectors become real and possess a symmetry center), we can split up (57) further to yield two polynomials of order $\frac{1}{2}M$ for even M and two polynomials of order $\frac{1}{2}(M-1)$ and $\frac{1}{2}(M+1)$ odd for M. This enables us to obtain explicit quadratic or biquadratic equations for the dependence of most band edges up to $M=8$ (and also for $M=12$) on the coupling integrals $U(10)$ and $U(01)$.

In Fig. 4 we plot the resulting bands for $M=5$. The right-hand bands correspond to $N=1$, $4[\phi\equiv\pm\frac{2}{5}\pi$ (mod $\times 2\pi)]$ and the left-hand bands refer to $N=2$, $3[\phi\equiv\pm\frac{4}{5}\pi$ (mod$2\pi)]$. The characteristic difference between both structures is the position of the first-order gap. For $N=1$, 4 the first-order gaps are those near the zero-field band edges; each separates a single subband from the others. For $N=2$, 3 the first-order gaps are those near the zero-field band center; each separates two subbands from the others. Going gradually from the tetragonal to the hexagonal case, we find that the upper first-order gaps are further widened, while the lower ones are narrowed.

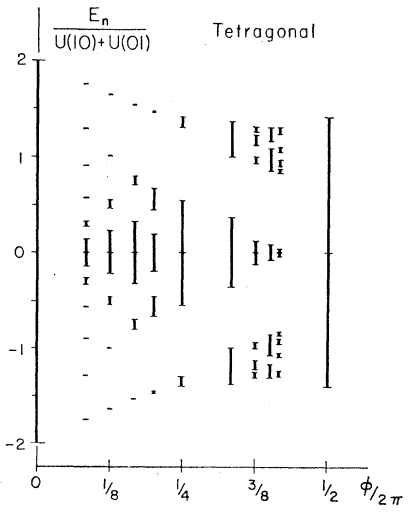

FIG. 5. Magnetic subbands for simple ratios $\phi/2\pi=N/M$ and tetragonal symmetry.

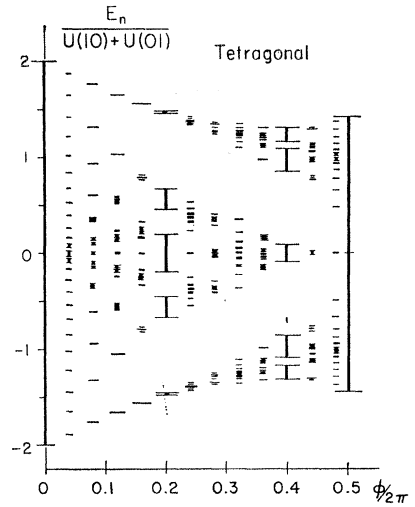

FIG. 6. Magnetic subbands for $M=25$, $N=1,\cdots,12$ and tetragonal symmetry.

In Fig. 5 we exhibit the subbands resulting in the tetragonal case $U(10)=U(01)$ for several simple values of ϕ, which allow an explicit representation of the roots of (57). Figure 5 shows that the subbands are arranged very regularly. They are very narrow at the edges of the zero-field band and broaden towards its center. The subbands obviously tend to form equidistant broadened Landau levels. The position of the subbands depends primarily on ϕ, while their width and structure depend on the rational ratio $\phi/2\pi=N/M$. Note the formation of groups of subbands, with the number of subbands per group being given by N. (Since the number of subbands equals M, and N and M have no common divisor, the number of subbands in the central group necessarily must differ from N.)

The largest over-all bandwidth corresponds to $\phi\equiv 0$ (mod2π), where it equals the zero-field bandwidth. Tending to move on the energy contours in k space the electrons do not fully realize their zero-field mobility normal to their magnetic orbit, except when the area of this orbit equals an integral multiple of the unit cell cross section.

For a further illustration of the above results, so as to include slightly more complicated values of ϕ, we calculated the band splitting for $M=25$ and $N=1,\cdots,12$ on a computer. The resulting structure is shown in Fig. 6. All the facts stated before turn out to be much more distinct. The broadening of the three lowest and the three highest levels for $\phi/2\pi=1/25$ is smaller by a factor of about 10^{-8} than their spacings. For $\phi/2\pi=2/25$, the bands as expected appear in pairs; the gaps between two consecutive pairs are 10^7 times larger than the tiny gaps between the two bands in the same pair. To indicate pairs, triplets, and quadruplets of subbands we have doubled, tripled, and quadrupled the length of the horizontal segments which denote their positions. Broad subbands occur whenever the rational representa-

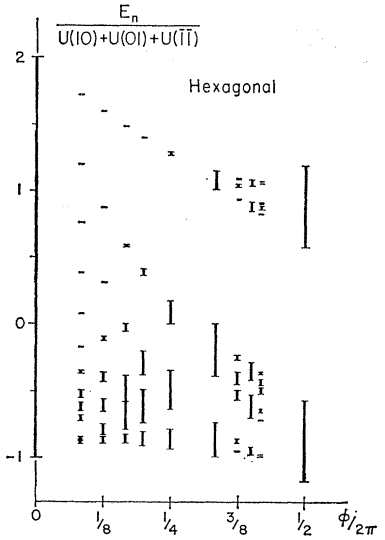

FIG. 7. Magnetic subbands for simple ratios $\phi/2\pi=N/M$ and hexagonal symmetry.

tion of $\phi/2\pi$ yields low integers N, M. The splitting for ϕ values close to these simple ratios is equidistant.

The switching on $U(\bar{1}\bar{1})$ brings about an important modification of the band splitting which is due to the fact that according to (54) even the first-order gap width $\det(\mu,\mu+1)$ depends on θ_1. This destroys the symmetry of the band structure with respect to $E_n=0$, so that in (57) even, and odd powers of E_n, occur simultaneously. The band edges are now obtained from

$$W(\theta_1,\theta_2)_{\rm ex} = \begin{cases} 2(-1)^N[|U(10)|^M+|U(01)|^M+|U(\bar{1}\bar{1})|^M] \\ (-1)^{N+1}[|U(10)U(01)/U(\bar{1}\bar{1})|^M+\text{cyclic}] \end{cases}. \quad (60)$$

A separation of (57) into two polynomials of order $\frac{1}{2}M$ [or $\frac{1}{2}(M-1)$ and $\frac{1}{2}(M+1)$] is again possible; the solution of the polynomial equation, however, is complicated by the presence of all powers of E_n up to $\frac{1}{2}M$.

Figures 7 and 8 exhibit the results of computer calculations for this hexagonal case. Figure 7 is similar to Fig. 5, and shows the band structure for some low values of M, while Fig. 8 once more gives the structure for $M=25$ and $N=1,\cdots,12$. Low values of M again yield relatively broad subbands. In the vicinity of these simple rational values, the subbands tend to form equidistant Landau levels. To be more exact, they tend to form equidistant levels at one edge of the broad subbands for low M values and equidistant pairs at the other. The pair formation is a consequence of the vanishing first-order interaction near the corresponding subband edge. The different translational behavior of the orbitals $|\theta_1\mu_2 n\rangle$ involved imposes a selection rule on the matrix elements induced by the lattice potential. The formation of equidistant levels and level pairs is most distinct close to $\phi\equiv 0(\text{mod}2\pi)$. Near one of the zero-field band edges two nearly degenerate eigenvectors of the secular determinant (54) exist, each one being different from zero only at one side of the extreme of $\det(\mu,\mu)$. The first-order gap near the opposite zero-field band edge, on the other hand, is broadened compared to the tetragonal case. This gap does not vanish even for $\phi/2\pi=\frac{1}{2}$. The second-order gap, which in the tetragonal case was limited by $\phi/2\pi=\frac{1}{4}$, is now extended to $\phi/2\pi=\frac{1}{2}$, etc.

VIII. LANDAU LEVEL STRUCTURE

So far we were mainly concerned with the tight-binding approach, i.e., we neither assumed the total

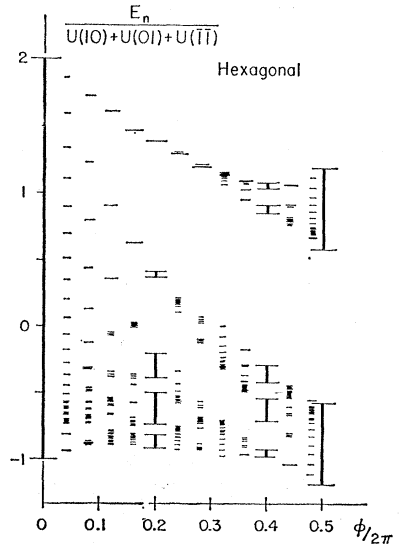

FIG. 8. Magnetic subbands for $M=25$, $N=1,\cdots,12$ and hexagonal symmetry.

bandwidth $2[U(10)+U(01)+U(\bar{1}\bar{1})]$ to change with B nor accounted for the characteristic dependence of the orbit lattice on B. Experimentally, available fluxes ϕ per unit cell of the real lattice reach, at best, values up to 10^{-3}, so that the limit of the tight-binding method is the extreme left of Figs. 5–8. In this region we find Landau levels whose width increases from the edges towards the center of the level system .Each level is represented by a goup of N out of a total of M subbands. The Landau levels near the band edges are equidistant. For the mean position of each group of subbands one obtains a generalization of previous results of Blackman,[16] of Harper,[2] and of Brailsford[3];

$$E_n(s)=\sum_\alpha U_{nn}(\alpha)-\phi(s+\tfrac{1}{2})[(\tfrac{1}{2}\sum_\alpha U_{nn}(\alpha))^2 - \sum_\alpha \tfrac{1}{2}U_{nn}^2(\alpha)]^{1/2} \quad (s=0,1,\cdots). \quad (61)$$

[16] M. Blackman, Proc. Roy. Soc. (London) **A166**, 1 (1938).

[Equation (61) does not apply to the level pairs arising in the hexagonal case.]

Turning to the nearly-free-electron scheme, we recall that the band index n is the quantum number of the Landau levels. We have to superpose the structure shown in Figs. 5–8 on each separate Landau level, noting that the equivalent for ϕ now is the flux $\tilde{\phi}$ through one cell of the orbit lattice. According to (46) and (48) we have

$$\tilde{\phi}=(1/B)(\mathbf{b}_1\times\mathbf{b}_2)_z=\mathbf{B}(\boldsymbol{\sigma}_1\times\boldsymbol{\sigma}_2). \tag{62}$$

Experimentally available fields now include a large number of periods: $\tilde{\phi}\gg 2\pi$. Using relation (3) between the real and reciprocal lattice vectors we find that

$$\frac{\tilde{\phi}}{2\pi}=\frac{1}{B}\frac{(\mathbf{b}_1\times\mathbf{b}_2)_z}{2\pi}=\frac{2\pi}{\mathbf{B}(\mathbf{a}_1\times\mathbf{a}_2)}=\frac{2\pi}{\phi}. \tag{63}$$

The flux through one cell of the orbit lattice divided by 2π is the reciprocal of the flux through one cell of the real lattice divided by 2π. From this reciprocity it follows that $\phi/2\pi$ and $\tilde{\phi}/2\pi$ simultaneously become rational. In the tight-binding case, $\phi/2\pi=N/M$ yields a splitting of each band into M subbands, arranged in groups of N, while in the nearly-free-electron method we find a splitting of each broadened Landau level into N sublevels due to $\tilde{\phi}/2\pi=M/N$. This means that the band structures produced by both methods agree totally, whenever the zero-field bands produced by both methods are alike.

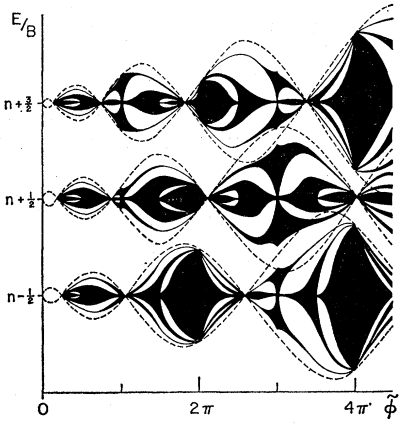

FIG. 9. Landau level structure.

Figure 9 shows the resulting structure of the Landau levels. As in Fig. 1, a nearest-neighbor approach is used, and $|\mathbf{b}_1|=|\mathbf{b}_2|$ is assumed. In the first step we ignore the subband splitting shown in Figs. 5–8, but superpose independently the broadenings caused by the different Fourier components $V(\mathfrak{g})$.

If we approximate the Laguerre polynomials as before, then we obtain the band edges shown by dashed lines in Fig. 9. These preliminary bands are split into subbands by the interference effect produced by the different components $V(\mathfrak{g})$, as shown in Figs. 5 and 6, and Figs. 7 and 8 for the tetragonal and hexagonal case, respectively. In Fig. 9 the tetragonal case is shown and only the first- and second-order gaps are actually displayed.

We did not calculate explicitly the effect of the interband interactions. However, much information is already contained in the above results: The one-dimensional potential used in Sec. IV yielded zero interaction between orbitals belonging to different gauge centers. Orbitals belonging to the same gauge center repel each other in second-order perturbation theory by an amount inversely proportional to their energy difference, so that the repulsion is stronger between narrow bands than between broad ones, and an effective level shift in the direction of increasing level broadening results. In the two-dimensional case treated in Sec. V we see from the general secular equation (50) that all orbitals belonging to the same value of θ_1 tend to repel each other. Since the labeling of orbitals by θ_1 alternates between adjacent subbands (see Fig. 2), each additional interaction must broaden the gaps and narrow the bands. This is also the effect of the interband interactions. As in the one-dimensional case the interband matrix elements are stricly correlated to the intraband matrix elements, by relations analogous to (38) and (39).

A lot of information about the interband interactions may also be obtained from the computer calculations of Sec. VII. We found each secular determinant (54) to yield a number of Landau levels, with N subbands per level for $\phi/2\pi=N/M$, which is just a multiband approach. The outer Landau levels (those near the zero-field band edges) of Figs. 6 and 8 show exactly the same substructure as those obtained in a one-band approximation. The inner levels (those near the zero-field band center) are comparatively broad and tend

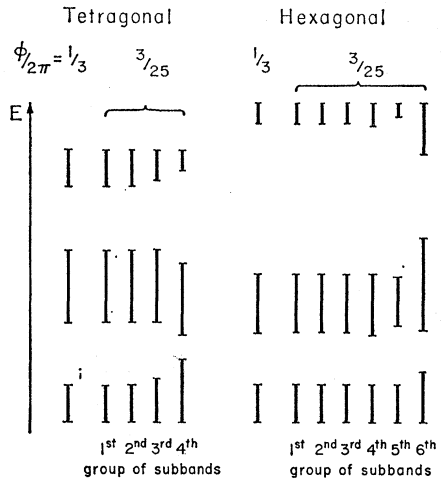

FIG. 10. Comparison of the level structures resulting from a one-band ($\phi/2\pi=\frac{1}{3}$) and a multiband ($\phi/2\pi=3/25$) approach. The hexagonal levels are alternatively inverted.

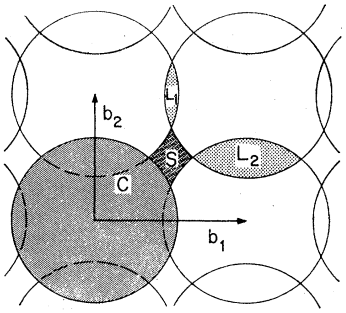

FIG. 11. Coupled Landau orbits.

to repel each other. This repulsion distorts them towards the center: The innermost level repels only imperfectly since it contains, as we saw before, fewer states. Figure 10 shows the structure of the Landau subbands obtained for $\phi/2\pi=3/25$ compared to the Landau level obtained for $\tilde{\phi}/2\pi=25/3=\frac{1}{3}$ (mod1). When the bandwidth is adjusted for the sake of comparison, the agreement between the two structures is perfect.

A similar splitting of the Landau levels for rational fluxes $\phi=2\pi N/M$ into N sublevels was obtained by Chambers.[9] He uses Pippard's model[8] and the one-dimensional model Hamiltonian proposed by Zak.[10] Though some features of his treatment coincide with those used here, he obtains at most two groups of subbands. This, as well as a lack of symmetry with respect to the lattice directions $\mathbf{a}_1$, $\mathbf{a}_2$, is due in his case to an incompatibility in the simultaneous use of asymmetric, periodic boundary conditions and independent switching parameters q_1, q_2.

IX. de HAAS-van ALPHEN AMPLITUDE

In order for the above structure (Fig. 9) to be observable in the de Haas-van Alphen or related effects it is necessary for the broadening of the Landau levels to be of the order of their spacing. This is just the condition which Reitz gave for magnetic breakdown.[12] Considering first the broadening we find Landau levels of modulated width to cross the Fermi energy as the field is varied. To obtain the frequencies of this modulation from (43)–(45) and (34), we use for the Laguerre polynomials an asymptotic expansion for fixed ratio of argument to order, namely,[13]

$$\exp\left(-\frac{\beta^2}{4B}\right)L_n\left(\frac{\beta^2}{2B}\right)=(-1)^n\frac{\sin[(n+\frac{1}{2})(2\theta-\sin2\theta)+\frac{1}{4}\pi]}{[\pi(n+\frac{1}{2})\sin2\theta]^{1/2}},\quad(64)$$

with $[2B(n+\frac{1}{2})]^{1/2}\cos\theta=\frac{1}{2}\beta$. The angle θ is conveniently interpreted by means of the quasiclassical electron orbits in k space attached to the Landau orbitals used. In Fig. 11 we plot four such orbits at adjacent lattice sites $\mathbf{0}$, $\mathbf{b}_1$, $\mathbf{b}_2$, $\mathbf{b}_1+\mathbf{b}_2$. θ is the angle between these orbits and the Brillouin-zone boundaries at $\pm\frac{1}{2}\boldsymbol{\beta}$, while $2B(n+\frac{1}{2})(2\theta-\sin2\theta)$ measures the area of overlap between adjacent orbits. The indication of areas in Fig. 11 we choose in accord with the notation of Chambers,[9] with the slight modification that our areas are defined in reciprocal space, while Chambers uses the orbit lattice. Applying (64) for $\mathbf{b}_1$ as well as for $\mathbf{b}_2$ we find the de Haas-van Alphen periods produced by the broadening to be

$$\Delta(1/B)=2\pi/L_1,\ 2\pi/L_2.\quad(65)$$

The lens orbits enclosing L_1 and L_2 do not yield quantized levels with spacing $L_{1,2}/2\pi B$, but modulate the Landau levels produced by the central circular orbits C [with the de Haas-van Alphen period $\Delta(1/B)=2\pi/C$] according to (65).

The structure of the broadened Landau is caused by orbitals actually including the two-dimensional variation of the potential (by those graphs shown in Fig. 3, which include a nonzero flux). The decisive variable for this structure is the flux $\tilde{\phi}$, so that also a periodic behavior in $1/B$ results, i.e.,

$$\Delta(1/B)=2\pi/|\mathbf{b}_1\times\mathbf{b}_2|.\quad(66)$$

However, the very short period given by (66) can hardly be detected in the de Haas-van Alphen effect. Physically one should observe first the hole orbit S (Fig. 11), which is related to the central orbit C, the lens orbits L_1 and L_2, and the reciprocal lattice cell by $|\mathbf{b}_1\times\mathbf{b}_2|=C-L_1-L_2+S$.

It is questionable whether even the Landau sublevel crossing of the Fermi energy could give rise to measurable de Haas-van Alphen oscillations. Figures 6 and 8 show these sublevels to be roughly equidistant only at values of $\tilde{\phi}$ close to zero (mod2π). The corresponding orbits thus enclose a very large number M of cells in k space, which gives rise to a probably unobservably large frequency in the magnetization. Similar conclusions on these hyperorbits were drawn earlier by Chambers and Pippard.[9]

The typical behavior of the de Hass-van Alphen susceptibility is shown in Fig. 12. With respect to the a_3 direction the free-electron-state density $N(E)\propto(E-E_n)^{1/2}$ has been assumed. The broadening of the Landau levels resulting from the central orbits C by the lens orbits L_1 and L_2 means that its amplitude is modified.

If the broadening were neglected, the contribution of the C-orbit quantization to the susceptibility would read in our notation[17]

$$\chi_{\rm osc}=\frac{C}{(2\pi)^2\sqrt{B}}\sum_{\nu=1}^{\infty}\frac{\sin[\nu C/B-(\nu+\frac{1}{4})\pi]2\pi^2\nu kT/B}{\nu^{3/2}\sinh[2\pi^2\nu kT/B]}.\quad(67)$$

[17] L. Landau, Proc. Roy. Soc. (London) **A170**, 363 (1959) (appendix to a paper by D. Shoenberg).

When the broadening is taken into account, Eq. (67) must be replaced by an expression which takes into account the new state density close to the Fermi energy. If we use the fact that the state density of each broadened Landau level in being that of a two-dimensional secular problem is approximately constant, we obtain instead of (67)

$$\chi_{\rm osc}=\frac{C}{(2\pi)^2\sqrt{B}}\sum_{\nu=1}^{\infty}\frac{\sin[\nu C/B-(\nu+\frac{1}{4})\pi]2\pi^2\nu kT/B}{\nu^{3/2}\sinh(2\pi^2\nu kT/B)}\times\frac{\sin\{(2\pi\nu/B)[U(10)+U(01)]\}}{\{(2\pi\nu/B)[U(10)+U(01)]\}}. \quad (68)$$

Each Fourier component is thus damped according to the ratio of the broadening to the spacing of the Landau levels near the Fermi energy. (This result is very similar to that obtained by Dingle[18] for a broadening of Landau levels resulting from collisions between the electrons.)

Figure 12 is drawn for the tetragonal case $U(10)=U(01)$; $U(\bar{1}\bar{1})=0$. The damping of the amplitude due to the lens orbits $L=L_1=L_2$ is indicated by the dashed lines. The contraction and splitting of the broadened Landau levels due to the hole orbits S intensifies the de Haas–van Alphen amplitude, thus yielding the heavy solid lines shown in Fig. 12. The level width for $\tilde{\phi}\equiv\pi$ (mod2π) is given by the level width for $\tilde{\phi}\equiv O$ (mod2π) times $\frac{1}{2}\sqrt{2}$, which yields only half the damping at $\tilde{\phi}\equiv\pi$ (mod2π) compared to $\tilde{\phi}\equiv O$ (mod2π).

The dash-dot line in Fig. 12 marks the center of the rapid oscillations due to the central orbits C. The position of this center is not affected by the level broadening and splitting in a one-band treatment, but is shifted due to the mutual repulsion of Landau levels in a multiband approach. Since in Sec. IV we proved that the shift of each Landau level by its adjacent levels is directly related to the respective level widths [Eqs. (38) and (39)], we find the center of the rapid de Haas–van Alphen oscillations (dash-dot line) to exhibit the same period $\Delta(1/B)=2\pi/L$ as the level broadening.

X. CONCLUSIONS

The simultaneous treatment of the tight-binding and of the nearly-free-electron method leads to a close agreement of the resulting subband (Landau level) structures. This agreement is guaranteed by the reciprocity of the fluxes ϕ and $\tilde{\phi}$ per unit cell of the real lattice and of the orbit lattice, respectively, $\phi/2\pi=(\tilde{\phi}/2\pi)^{-1}$. Whenever $\phi/2\pi$ takes a ratio N/M (with $N\ll M$ because of $\phi/2\pi\ll 1$ for all experimentally available fluxes), the tight-binding method yields M subbands, arranged regularly into groups of N subbands. Each group corresponds to one Landau level. Their width increases from the edges towards the center of the level system. The central groups are in general short of subbands owing to the fact that M/N is not an integer. The nearly-free-electron method, in agreement with this, results in a splitting of each Landau level into N sublevels, since $\tilde{\phi}/2\pi=M/N$ and $M\gg N$. The level structure agrees exactly with that obtained in the tight-binding case, as demonstrated in Fig. 10. The level width is proportional to the overlap between adjacent Landau orbitals in the orbit lattice.

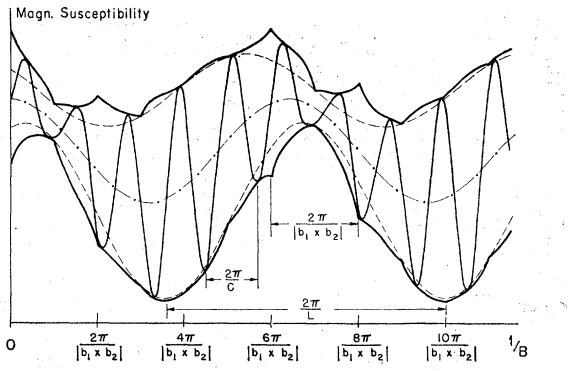

FIG. 12. de Haas–van Alphen oscillations.

This close agreement of the substructures resulting from both the tight-binding and the nearly-free-electron methods shows that the essential condition for these methods to give identical results is the agreement of the zero-field band structures. Once this is achieved, Landau level broadening and structure are obtained more conveniently by means of the nearly-free-electron method. The broadening of a level at the energy $E_n=B(n+\frac{1}{2})$ can be interpreted by Bragg reflections of the corresponding quasiclassical orbit at the lattice potential. This relates the broadening to the zero-field energy structure in k space, and is the basis for Pippard's[7,8] treatment of the broadening. The broadening is given by the overlap integral between adjacent orbits in k space times the respective Fourier component of the lattice potential. It increases exponentially when these orbits approach the Brillouin-zone boundaries, and oscillates with an amplitude proportional to $1/\sqrt{E_n}$ in the overlap region. The period of these oscillations is given by 2π times the ratio of wave numbers to reflection vector with respect to the level index n, and by $2\pi/$(area of overlap) with respect to the reciprocal field. The crossing of these modulated levels through the Fermi surface as the field is varied gives rise to corresponding de Haas–van Alphen oscillations. The structure of the broadened levels is caused by orbits, in which an electron is Bragg-reflected by at least two independent vectors β. Since the decisive parameter for this structure is the flux $\tilde{\phi}$, de Haas-van Alphen oscillations measuring the area of the hole orbits in Fig. 11 result.

However, the nearly-free-electron method fails to provide the correct variations of the level spacing or even to predict the usual nonmagnetic gaps without application of a higher-order perturbation treatment.

[18] R. B. Dingle, Proc. Roy. Soc. (London) **A211**, 517 (1952).

These effects are more appropriately derived by the tight-binding method, which in addition to the splitting of each zero-field band into subband groups (Landau levels) yields clearly marked low-order gaps. (Compare the first- and second-order magnetic gaps in Figs. 6 and 8.) The position of the subband groups is given by the flux ϕ, and their structure is determined by the ratio $\phi/2\pi=N/M$. From counting the total number of states we conclude that all magnetic gaps are crossed by single levels between any two rational values of $\phi/2\pi$: The number of states at energies above the first-order gap in Figs. 6 and 8 is just $\phi/2\pi$ times the total number of states. Still, the state density in the magnetic gaps is strictly zero. Indications suggesting a similar formation of low-order gaps within the nearly-free-electron method are obtained from the second-order perturbation treatment performed in Sec. IV. The mutual repulsion of Landau levels is strictly correlated to their broadening, i.e., they are pushed towards the energy direction with increasing broadening.

Note added in proof: The level structure corresponding to the tetragonal tight-binding case [i.e., the level structure resulting from the fundamental determinant (51) for $U(\pm 1\ 0)=U(0\ \pm 1)\neq 0$, $U(\mu_1\mu_2)=0$ otherwise] has recently been treated numerically by Butler and Brown.[19] In addition to the qualitative level scheme given for this case in the concluding section of Ref. 4, Butler and Brown obtain a subband structure equivalent to that shown in Figs. 5 and 6. This renders important further support of the results given in Secs. VI and VII of this paper.

ACKNOWLEDGMENTS

The author wishes to thank Professor L. M. Falicov for stimulating discussions and criticisms of this work, and him as well as J. Ruvalds for some helpful remarks on the manuscript. He also wants to thank the staff of the James Franck Institute for their kind hospitality.

[19] F. A. Bulter and E. Brown, Phys. Rev. **166**, 630 (1968).